PHYSICAL REVIEW B **79**, 174420 (2009)

Ferroelectric poling and converse-piezoelectric-effect-induced strain effects in $La_{0.7}Ba_{0.3}MnO_3$ thin films grown on ferroelectric single-crystal substrates

R. K. Zheng,[1,*] Y. Jiang,[1] Y. Wang,[1] H. L. W. Chan,[1,†] C. L. Choy,[1] and H. S. Luo[2]
[1]*Department of Applied Physics and Materials Research Center, The Hong Kong Polytechnic University, Hong Kong, China*
[2]*State Key Laboratory of High Performance Ceramics and Superfine Microstructure, Shanghai Institute of Ceramics, Chinese Academy of Sciences, Shanghai 201800, China*

(Received 1 January 2009; revised manuscript received 13 April 2009; published 14 May 2009)

Using ferroelectric $0.67Pb(Mg_{1/3}Nb_{2/3})O_3$-$0.33PbTiO_3$ single crystals as substrates, we studied the effects of the ferroelectric poling and the converse piezoelectric effect on the strain state, resistance, insulator-to-metal transition temperature (T_C), and magnetoresistance (MR) of $La_{0.7}Ba_{0.3}MnO_3$ (LBMO) thin films. *In situ* x-ray diffraction measurements indicate that the ferroelectric poling (or the converse piezoelectric effect) induces a substantial reduction in the in-plane tensile strain in the LBMO film, giving rise to a decrease in the resistance and an increase in T_C. The relative changes of the resistance and T_C are proportional to the induced reduction in the in-plane tensile strain ($\delta\varepsilon_{xx}$) in the film. The reduction in the in-plane tensile strain leads to opposite effects on MR below and above T_C, namely, MR is reduced for $T<T_C$ while MR is enhanced for $T>T_C$. We discuss these strain effects within the framework of the Jahn-Teller (JT) electron-lattice coupling and phase separation scenario that are relevant to the induced strain. Similar studies on $CaMnO_3$ thin films, for which there is no JT distortion of MnO_6 octahedra, show that the resistance of the films also decreases when the tensile strain is reduced, indicating that the resistance change arising from the reduction in Mn-O bond length dominates over that arising from the reduction in Mn-O-Mn bond angle.

DOI: 10.1103/PhysRevB.79.174420 PACS number(s): 75.47.Lx, 75.47.Gk, 77.22.Ej, 77.65.−j

I. INTRODUCTION

In the last decade, much effort has been devoted to colossal magnetoresistance (CMR) manganite thin films due to their interesting physical properties and possible device applications. A number of experimental studies and theoretical calculations have undoubtedly shown that the substrate-induced strain can drastically influence a variety of properties of manganite thin films, such as the insulator-to-metal transition temperature (T_C) (Ref. 1), magnetoresistance (MR),[2] magnetic anisotropies,[3] phase separation,[4] and charge/orbital ordering.[5] Therefore, a comprehensive and quantitative study of the intrinsic strain dependence of film properties is very important from both the fundamental and technological viewpoints.

Recently, it was reported that an in-plane compressive strain reduces ferromagnetism and T_C while a tensile strain enhances ferromagnetism and T_C in low-doped $La_{1-x}Ba_xMnO_3$ ($0.05 \leq x \leq 0.2$) thin films.[6,7] These strain effects are different from the usual results observed in other CMR systems, e.g., $La_{0.9}Sr_{0.1}MnO_3$, where a compressive strain enhances ferromagnetism and T_C (Ref. 8). Kanki *et al.*[7] proposed that an increase in charge carrier transfer resulting from the strain-induced modification of Mn-O-Mn networks rather than an increase in charge carrier density is responsible for the strain effect in $La_{1-x}Ba_xMnO_3$ films. In contrast, Murugavel *et al.*[9–11] found that, irrespective of whether the substrate-induced strain is compressive or tensile, oxygen nonstoichiometry strongly affects the hole-doping level, strain state, and the transport properties of $La_{1-x}Ba_xMnO_3$ ($x=0.08, 0.2$) films. Orgiani *et al.*[12] studied the role of oxygen content on the transport properties of $La_{0.7}Ba_{0.3}MnO_3$ (LBMO) films and found that the oxygen content strongly influences the strain state and transport properties of the films. These results strongly indicate that, in addition to the substrate-induced strain, oxygen content plays a very important role in determining the electrical, magnetic, and structural properties of $La_{1-x}Ba_xMnO_3$ thin films.

Ferroelectric $(1-x)Pb(Mg_{1/3}Nb_{2/3})O_3$-$xPbTiO_3$ (PMN-xPT) single crystals with compositions near the morphotropic phase-boundary region exhibit large remnant ferroelectric polarization ($P_r=30\sim35$ $\mu C/cm^2$), low coercive field, and excellent piezoelectric activity ($d_{33}>1500$ pC/N).[13] PMN-xPT has a perovskite structure with lattice constants $a\sim b\sim c\sim4.02$ Å (Ref. 13), which are close to those of $Pb(Zr_{0.52}Ti_{0.48}O_3)$ ($a=4.04$ Å, $c=4.11$ Å) (Ref. 14) and $BaTiO_3$ ($a=3.99$ Å, $c=4.03$ Å).[15] Because of the good ferroelectric, piezoelectric, and structural properties of PMN-xPT single crystals, they are very good materials for use as ferroelectrically and piezoelectrically active substrates. Recently, Gangineni *et al.*,[16] Thiele *et al.*,[17,18] and Zheng *et al.*[19–21] have successfully grown perovskite $La_{1-x}A_xMnO_3$ (A=Ca, Sr) thin films on PMN-xPT ($x\sim0.28, 0.33$) substrates, and have demonstrated that the strain state of these films can be reversibly controlled via the converse piezoelectric effect of the substrates. This approach opens the possibility that the intrinsic effects of the substrate-induced strain on the properties of films can be studied without introducing the effects of extrinsic variables, e.g., crystalline quality, disorder, and oxygen nonstoichiometry.

In order to attain a detailed and quantitative understanding of the substrate-induced strain effects in $La_{1-x}Ba_xMnO_3$ films, in this paper, we used ferroelectric $0.67Pb(Mg_{1/3}Nb_{2/3})O_3$-$0.33PbTiO_3$ (PMN-PT) single crystals as substrates and studied the effects of substrate-induced strain on the strain state, resistance, T_C, and magnetotransport properties of LBMO films by *in situ* inducing a strain in the film via the ferroelectric poling or the converse piezo-

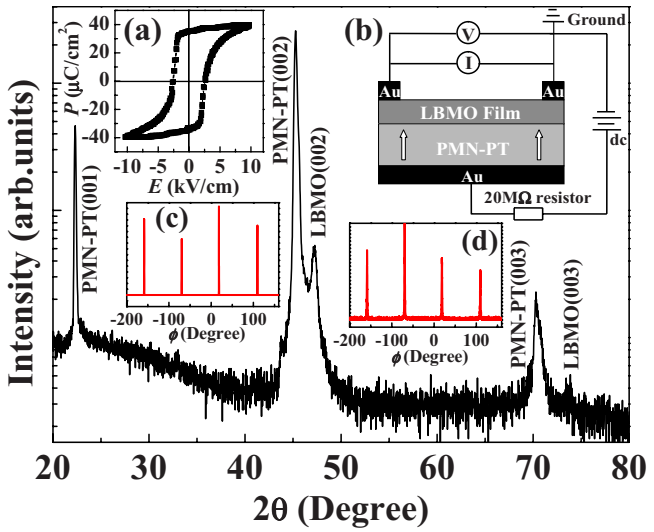

FIG. 1. (Color online) X-ray diffraction pattern of the LBMO/PMN-PT structure. The inset (a) shows the polarization electric-field hysteresis loop of the PMN-PT substrate measured at 296 K. The inset (b) shows a schematic diagram of the LBMO/PMN-PT structure and the electrical measurement circuit. The arrow in the inset (b) represents the polarization direction. The insets (c) and (d) show the XRD ϕ scans on the PMN-PT(101) and LBMO(101) reflections, respectively.

electric effect. The experimental results indicate that, associated with the ferroelectric poling, the in-plane tensile strain in the film was reduced by ~0.27%, giving rise to a decrease in the resistance in the temperature range from 78 to 325 K and an increase of T_C by ~12.6 K. At the same time, MR in the ferromagnetic (FM) state is reduced while MR in the paramagnetic (PM) state is enhanced. These induced strain effects are found to be closely related to the phase separation and the Jahn-Teller (JT) electron-lattice coupling linked to the induced reduction in the in-plane tensile strain in the film.

II. EXPERIMENTAL DETAILS

We have grown the PMN-PT single crystals by a modified Bridgman technique.[22] Ferroelectric measurements using a standard Sawyer-Tower circuit driven with 1 Hz sinusoidal pulse electric field showed that the single crystals exhibited a sharp polarization hysteresis loop with a remnant polarization close to 33 $\mu C/cm^2$ and a coercive field (E_C) close to 2.5 kV/cm [inset (a) of Fig. 1]. These crystals were cut into small plates with the plate normal in the ⟨001⟩ crystal direction and polished to a surface roughness less than 1 nm. LBMO films were deposited on the (001)-oriented and polished PMN-PT substrates using dc magnetron sputtering. The deposition was carried out in an argon-oxygen flow with 60% Ar and 40% O_2 at a pressure of 5 Pa, and a substrate temperature of 700 °C. After deposition, the films were cooled to room temperature and then postannealed in 1 atm of flowing O_2 at 700 °C for 30 min using a rapid thermal processor furnace. Since the lattice constants ($a \sim b \sim c \sim 3.916$ Å) of LBMO bulk material[23] are smaller than those ($a \sim b \sim c \sim 4.02$ Å) of the PMN-PT substrate in unpoled state (referred to as P_r^0), it is estimated that LBMO films grown on PMN-PT substrates would be subjected to an in-plane tensile strain. The thicknesses of these films were measured by field-emission scanning electron microscopy to be ~65 nm. X-ray diffraction (XRD) patterns of the PMN-PT substrate and the LBMO film were recorded using a Bruker D8 Discover x-ray diffractometer when a dc electric field E ($0 \leq E \leq 10$ kV/cm) was applied to the LBMO/PMN-PT structure. The films were highly (001) oriented and no secondary phases were found, as shown in Fig. 1. XRD ϕ scans on the PMN-PT(101) and LBMO(101) reflections were also performed. A fourfold symmetry is clearly seen for both the PMN-PT substrate and the LBMO film [insets (c) and (d) of Fig. 1, respectively], which is an indication of the cube-on-cubic epitaxial growth of the LBMO film on the PMN-PT substrate.

The resistance of the LBMO films was measured using the electrical measurement circuit shown in the inset (b) of Fig. 1. A constant current of 5 μA was applied to the thin film through the two top-top gold electrodes using a Keithley Model 2400 source meter with input resistance >10 GΩ and the voltage difference between the two top-top gold electrodes was measured by a Keithley Model 2000 digital multimeter. The PMN-PT substrate was poled by applying a poling field E (much larger than E_C) to the LBMO/PMN-PT structure through the top and bottom gold electrodes using a Keithley Model 6517A electrometer, and the same measurement circuit shown in the inset (b) of Fig. 1. Note that the top and bottom gold electrodes were always held at low and high potentials, respectively. We point out that the ferroelectric field effect present at the LBMO/PMN-PT interface has a negligible influence on the transport properties since the screening length of the electric field is less than few unit cells,[18,24] which is smaller than the thickness (~65 nm) of the LBMO films. The resistance of the PMN-PT substrate is estimated to be ~5.4 GΩ cm under $E=10$ kV/cm, obtained by measuring the leakage current in the PMN-PT substrate. Using a Model 7600 Lakeshore Hall measurement system, MR of the films was measured when a magnetic field was applied parallel to the film plane. Magnetic measurements were performed with a Model 7600 Lakeshore vibrating sample magnetometer.

III. RESULTS AND DISCUSSION

A. $La_{0.7}Ba_{0.3}MnO_3$/PMN-PT structure

1. Effects of strain induced by ferroelectric substrate poling on the film resistance

In order to observe the effects of the strain induced by ferroelectric poling on the strain state and transport properties of the LBMO film, we measured the resistance of the film between the two top-top gold electrodes as a function of the electric field E applied to the LBMO/PMN-PT structure through the top (held at low potential) and bottom gold electrodes (held at high potential) at a fixed temperature of 296 K. Note that the initial polarization state of the PMN-PT substrate was P_r^0 and E was increased from 0 to +10 kV/cm

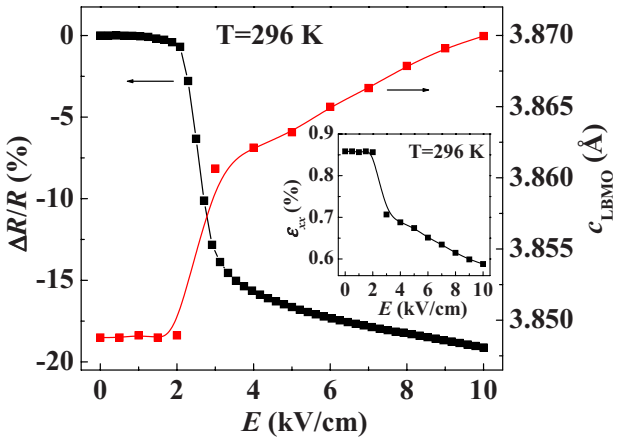

FIG. 2. (Color online) Relative change of the resistance and the *c*-axis lattice constant of the LBMO film at 296 K as a function of E applied to the LBMO/PMN-PT structure. The initial polarization state of the PMN-PT substrate is P_r^0. The inset shows the in-plane strain ε_{xx} of the film at 296 K as a function of E applied to the LBMO/PMN-PT structure.

in steps of 0.21 kV/cm. The relative change of the resistance due to the ferroelectric poling, $\Delta R/R$, is plotted as a function of E in Fig. 2. Here, $\Delta R/R$ is defined as $\Delta R/R=[R(E)-R(0)]/R(0)$, where $R(E)$ and $R(0)$ are the resistance of the film under an electric field E and zero electric field, respectively. It can be seen that the resistance decreases slightly by 0.7% for $E \leq 2.1$ kV/cm, which could be due to the partial poling of the PMN-PT substrate. It is worth noting that the resistance decreases drastically with increasing E from 2.1 to 3 kV/cm and decreases gently with further increase in E. We found that, after the measurements of the resistance as a function of E, the PMN-PT substrate had a piezoelectric coefficient d_{33} of 1900 pC/N which indicates that the PMN-PT substrate had been poled very well. Moreover, the drastic decrease in the resistance occurs near $E \sim 2.5$ kV/cm, which is close to the coercive field of the PMN-PT substrate. Therefore, it is reasonable to conclude that the decrease in the resistance induced by the electric field is associated with the ferroelectric poling in the PMN-PT substrate, which could consequently modify the strain state and transport properties of the LBMO film.

To clarify this point, we measured the out-of-plane or *c*-axis lattice constant of the film by *in situ* measuring the position of LBMO(002) reflection during the application of an electric field E ($0 \leq E \leq 10$ kV/cm) to the LBMO/PMN-PT structure in steps of 1 kV/cm. Note that the PMN-PT substrate is initially in P_r^0 state. In Fig. 2, we show the *c*-axis lattice constant of the film as a function of E. When the PMN-PT substrate is in P_r^0 state, i.e., $E < 2$ kV/cm, the *c*-axis lattice constant is about 3.849 Å. This value is smaller than that (i.e., $c=3.916$ Å) of $La_{0.7}Ba_{0.3}MnO_3$ bulk material,[23] indicating that the film is under an out-of-plane compressive ($\varepsilon_{zz}=-1.71\%$) and an in-plane tensile strain. For $E \leq 2$ kV/cm, the *c*-axis lattice constant remains almost unchanged with increasing E but increases drastically with increasing E from 2 to 3 kV/cm and then increases monotonously for $E > 3$ kV/cm. For an unpoled ferroelectric material, it is expected that the application of an electric field would induce a nonlinear change in the lattice constants (or strain) in the material. The observed electric-field-induced nonlinear change in the *c*-axis lattice constant of the LBMO film is apparently due to the strain induced by the ferroelectric poling in the PMN-PT substrate, giving direct evidence that ferroelectric poling is responsible for the decrease in the resistance of the film. We note that, when $E=10$ kV/cm is applied to the LBMO/PMN-PT structure, the *c*-axis lattice constant increases to 3.870 Å, which is smaller than that of $La_{0.7}Ba_{0.3}MnO_3$ bulk material, indicating that the film is still under in-plane tensile strain. The in-plane tensile strain ε_{xx} is related to the out-of-plane compressive strain ε_{zz} by the expression $\varepsilon_{zz}=-(2\nu/1-\nu)\varepsilon_{xx}$, where ν is the Poisson's ratio. Using $\nu=0.5$ (i.e., volume-preserving distortion) for the LBMO film,[25] ε_{xx} is calculated and plotted as a function of E in the inset of Fig. 2. As E increases from 0 to 10 kV/cm, ε_{xx} decreases from 0.86% to 0.59%, corresponding to a relative reduction of ε_{xx} by ~31%. The evolution of ε_{xx} with E is in good agreement with that of the transport behavior, which strongly indicates that the decrease in the resistance is due to the reduction in the in-plane tensile strain induced by the ferroelectric poling.

A reduction in the in-plane tensile strain would reduce the tetragonal distortion of the MnO_6 octahedra in the film and hence modify the JT electron-lattice coupling strength.[7,26–29] At $E=0$ kV/cm (i.e., the PMN-PT substrate is in P_r^0 state), the film is subjected to an in-plane tensile strain ($\varepsilon_{xx}=0.86\%$), implying that the MnO_6 octahedra are compressed along *c* axis and elongated in the film plane.[29] Such tetragonal distortion of the MnO_6 octahedra would localize the charge carriers due to the JT electron-lattice coupling. At $E=10$ kV/cm, ε_{xx} is reduced to 0.59%, indicating that the tetragonal distortion of the MnO_6 octahedra has been significantly reduced. This would reduce the JT electron-lattice coupling strength, thereby favoring the delocalization and hopping of charge carriers.[7,26,27]

2. Effects of strain induced by the converse piezoelectric effect on the film resistance

After the PMN-PT substrate had been positively polarized (i.e., electric dipole moments in the PMN-PT substrate point toward the LBMO film, referred to as P_r^+), we studied the effects of the strain induced by the converse piezoelectric effect on the strain state, T_C, and transport properties of the LBMO film. In Fig. 3, we show the temperature dependence of the resistance for the LBMO film when dc electric fields of 0, 2.5, 5, 7.5, and 10 kV/cm is applied to the LBMO/PMN-PT structure, respectively. Note that the resistance was measured using the electrical measurement circuit shown in the inset (b) of Fig. 1. During the measurements the top and bottom gold electrodes were held at low and high potentials, respectively, so that the direction of the electric field is the same as that of the polarization. With increasing E from 0 to 10 kV/cm, the resistance decreases over the entire temperature range, with the decrease being particularly noticeable near T_C. We found that, whether the film is in the high-temperature insulating state (e.g., 296 K), low-temperature metallic state (e.g., 78 K), or at T_C (i.e., 273 K), the relative change in the resistance ($\Delta R/R$) at a fixed temperature de-

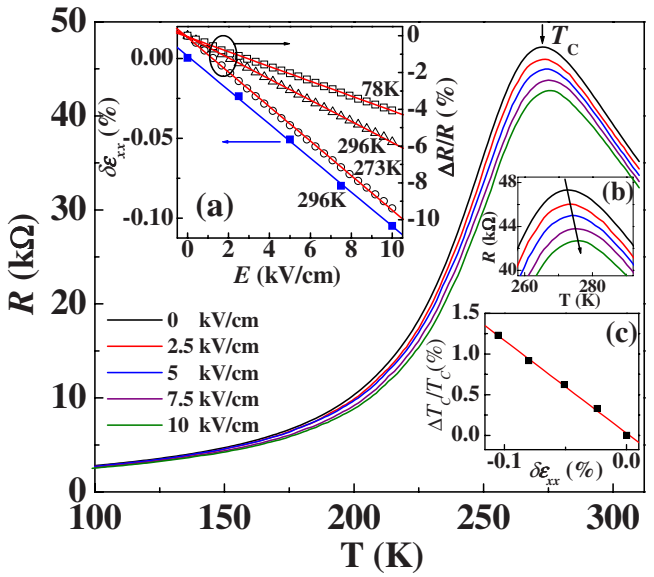

FIG. 3. (Color online) Temperature dependence of the resistance for the LBMO film when a dc electric field E is applied to the LBMO/PMN-PT structure after the PMN-PT substrate had been polarized to P_r^+ state. The inset (a) shows the relative change of the resistance, $\Delta R/R$, and the induced reduction in the in-plane tensile strain, $\delta\varepsilon_{xx}$, of the LBMO film versus E. The inset (b) shows an expanded view of the temperature dependence of the resistance near T_C. The inset (c) shows $\Delta T_C/T_C$ as a function of $\delta\varepsilon_{xx}$.

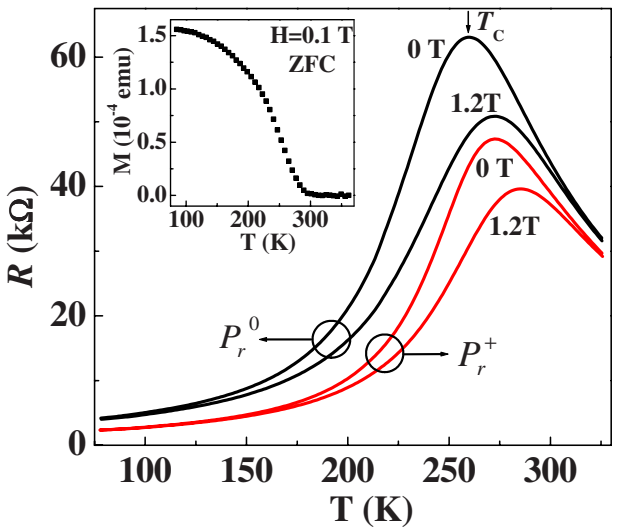

FIG. 4. (Color online) Temperature dependence of the resistance for the LBMO film under $H=0$ and 1.2 T when the PMN-PT substrate is in P_r^0 and P_r^+ states, respectively. The inset shows the temperature dependence of the zero-field-cooled magnetization (M) for the LBMO film when the PMN-PT substrate is in P_r^0 state.

creases linearly with increasing E [inset (a) of Fig. 3]. It is known that, for a ferroelectric material, the strain induced by the converse piezoelectric effect is proportional to the electric field E applied to the material. *In situ* XRD measurements on the LBMO/PMN-PT structure indicate that both the c-axis lattice constant of the PMN-PT substrate and the LBMO film increases linearly with increasing E (not shown here), indicating that the strain induced in the film is due to the converse piezoelectric effect in the PMN-PT substrate.[17–21] Using the expression $\varepsilon_{zz}=-(2\nu/1-\nu)\varepsilon_{xx}$ and putting $\nu=0.5$ for the LBMO film,[25] the induced reduction in the in-plane tensile strain $\delta\varepsilon_{xx}$ [in comparison with the strain state when $E=0$ kV/cm, i.e., $\delta\varepsilon_{xx}=\varepsilon_{xx}(E)-\varepsilon_{xx}(0)$] is calculated and plotted as a function of E in the inset (a) of Fig. 3. It is clear that $\delta\varepsilon_{xx}$ is linearly dependent on E, thus implying that $\Delta R/R$ is proportional to the induced reduction in the in-plane tensile strain ($\delta\varepsilon_{xx}$). The relationship between $\Delta R/R$ and $\delta\varepsilon_{xx}$ can be written as $\Delta R/R=m\delta\varepsilon_{xx}$, where m is a constant.

We note that, associated with the reduction in the in-plane tensile strain, T_C increases linearly with increasing E as shown in the inset (b) of Fig. 3. Since the reduction in the in-plane tensile strain $\delta\varepsilon_{xx}$ is proportional to E, the relationship between T_C and $\delta\varepsilon_{xx}$ can be expressed as $T_C(E)=T_C(0)+p\delta\varepsilon_{xx}$, where p is a negative constant and $\delta\varepsilon_{xx}$ has a negative value. Thus, the relationship between $\Delta T_C/T_C$ and $\delta\varepsilon_{xx}$ can be expressed as $\Delta T_C/T_C=q\delta\varepsilon_{xx}$, where q is a negative constant, so $\Delta T_C/T_C$ is proportional to $\delta\varepsilon_{xx}$ [inset (c) of Fig. 3]. The T_C-$\delta\varepsilon_{xx}$ coefficient $\Delta T_C/T_C/\delta\varepsilon_{xx}$ is found to be 11.4 here, which implies that a change in the in-plane strain by 1% would induce a 11.4% shift in T_C. This is consistent with the theoretical calculations by Millis *et al.*[27] who showed that a change in the in-plane biaxial strain by 1% would cause a 10% shift in T_C, and thus provides evidence for the important role of the JT electron-lattice coupling linked to substrate-induced strain in the LBMO film.

3. Changes in film magnetoresistance due to strain induced by ferroelectric substrate poling

Figure 4 shows the temperature dependence of the resistance for a LBMO film under zero magnetic field and a magnetic field of $H=1.2$ T when the PMN-PT substrate is in P_r^0 and P_r^+ state, respectively. When the PMN-PT substrate is in P_r^0 state, the resistance of the film increases with decreasing temperature from 325 K and undergoes an insulator-to-metal transition at $T_C\sim260$ K. As the magnetic field H increases from 0 to 1.2 T, T_C increases from 260 to 272.6 K and the resistance decreases over the entire temperature range. Associated with the insulator-to-metal transition, the film shows a paramagnetic-to-ferromagnetic phase transition (see inset of Fig. 4).

As shown in Fig. 4, at $H=0$ T, after the PMN-PT substrate has been polarized to P_r^+ state, T_C increases from 260 to 272.5 K and the resistance decreases over a wide temperature range from 77 to 325 K. These changes in the transport behavior of the LBMO film induced by ferroelectric poling are qualitatively consistent with those observed in $La_{0.75}Ca_{0.25}MnO_3$/PMN-PT (Ref. 20), $La_{0.7}Sr_{0.3}MnO_3$/PMN-PT (Ref. 21), and $La_{0.85}Ba_{0.15}MnO_3$/PMN-PT (Ref. 30) structures. When a field of $H=1.2$ T is applied, T_C increases further to 285 K and the resistance is further reduced.

The values of MR at $H=1.2$ T when the PMN-PT substrate is in P_r^0 and P_r^+ states were calculated from the data in Fig. 4 and shown in Fig. 5. It is interesting to see that the two MR versus T curves have a crossover near T_C, indicating that

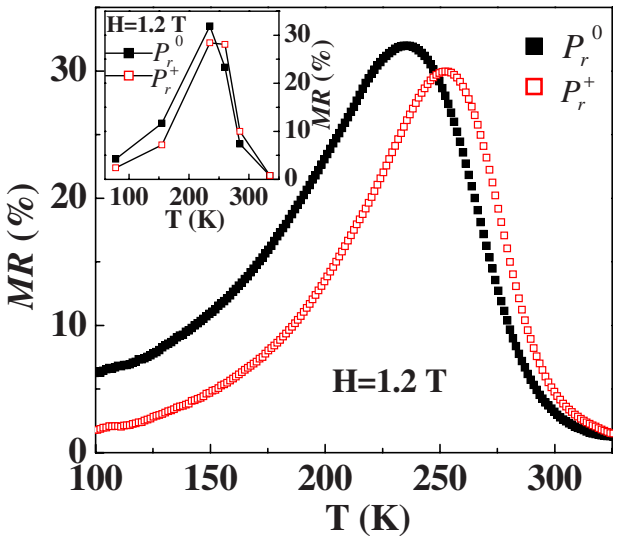

FIG. 5. (Color online) Temperature dependence of MR (MR $=[R(0)-R(H)]/R(0)$) of the film under $H=1.2$ T when the PMN-PT substrate is in P_r^0 and P_r^+ states, respectively. The inset shows MR derived from Fig. 6 as a function of temperature when the PMN-PT substrate is in P_r^0 and P_r^+ states, respectively.

a reduction in the in-plane tensile strain leads to an increase in MR in the PM state but a decrease in MR in the FM state. To confirm this strain effect on MR, we measured MR of the film at various fixed temperatures covering the range from the FM state to the PM state. In Fig. 6, we show MR versus H curves at several temperatures when the PMN-PT substrate is in P_r^0 and P_r^+ states, respectively. The results clearly indicate that, in comparison with the MR when the PMN-PT substrate is in P_r^0 state, the MR value when the PMN-PT substrate is in P_r^+ state is reduced in the FM state (e.g., 78, 155, and 235 K) but enhanced in the PM state (e.g., 260, 285, and 335 K). We plotted MR at $H=1.2$ T (derived from Fig. 6) for both P_r^0 and P_r^+ states as a function of temperature in the inset of Fig. 5. The two MR versus T curves also show a crossover, consistent with the behavior of the MR shown in Fig. 5.

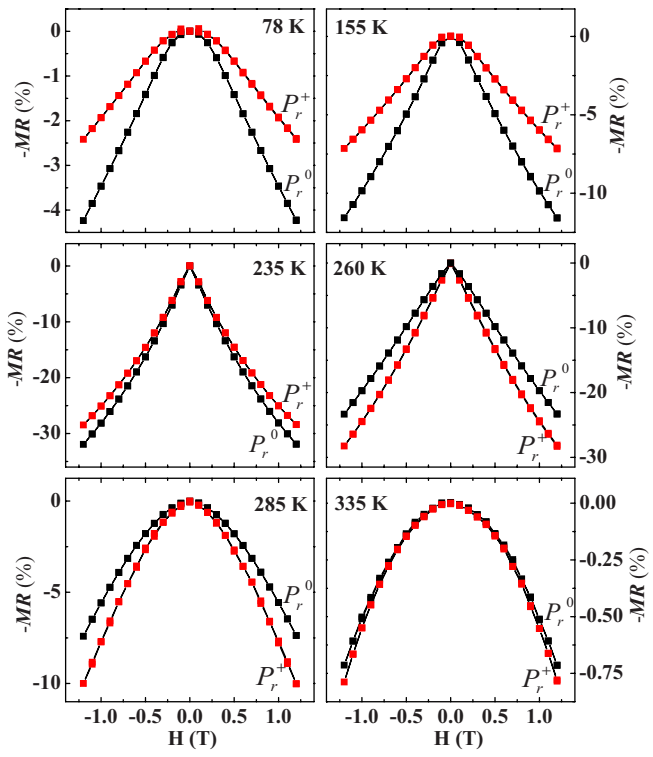

FIG. 6. (Color online) MR versus H curves at several temperatures for the LBMO film when the PMN-PT substrate is in P_r^0 and P_r^+ states, respectively.

A number of experimental studies and theoretical calculations have shown that the magnetotransport properties of manganite thin films are closely associated with coexisting PM insulating and FM metallic phases, i.e., the phase separation.[1,4,31–33] It is usually observed that MR has a maximum close to T_C, where the PM insulating phase and the FM metallic phase coexist and strongly compete with each other. At T_C, small external perturbations, e.g., magnetic field, would modify the subtle balance between these two phases, resulting in a large MR. In the high temperature PM insulating state, the PM insulating phase dominates over the FM metallic phase. Thus, the competition between the PM insulating phase and the FM metallic phase for $T>T_C$ is weaker than that at T_C. As discussed above, the reduction in the tensile strain induced by the ferroelectric poling reduces the JT electron-lattice coupling strength, favoring the active hopping of e_g electrons. Therefore, the volume fraction of the FM metallic phase would increase at the expense of that of the PM insulating phase, which would enhance MR. In the low temperature FM metallic state, the competition between the PM insulating phase and the FM metallic phase is weaker than that at T_C because the volume fraction of the FM metallic phase dominates over the PM insulating phase. Again, the reduction in the JT electron-lattice coupling strength induced by the ferroelectric poling would reinforce the FM metallic state, which would suppress MR. Therefore, if the phase-separation scenario relevant to the strain induced by the ferroelectric poling is taken into account, the opposite effects of the induced strain on the MR in the LBMO film can be reasonably understood.

B. $CaMnO_3$/PMN-PT structure

To obtain insight into the effects of induced strain on the Mn-O bond length and/or the Mn-O-Mn bond angle, we studied the effects of strain induced by the ferroelectric poling and the converse piezoelectric effect on the transport properties of $CaMnO_3$ (CMO) thin films grown on PMN-PT substrates. $CaMnO_3$ films were chosen because they do not exhibit JT distortions so the effects of JT electron-lattice coupling on the transport properties can be neglected. XRD measurements indicated that, associated with the switching of the poling state from P_r^0 to P_r^+, the PMN-PT(002) and CMO(002) reflections shift to lower 2θ angles, as shown in the inset (a) of Fig. 7. As a result, the c-axis lattice constant of the $CaMnO_3$ film increases from 3.709 to 3.717 Å, with the latter value still smaller than the lattice constant (i.e., 3.727 Å) of the $CaMnO_3$ bulk material.[34] Assuming a Poisson's ratio of $\nu=0.5$ for the $CaMnO_3$ film, the in-plane ten-

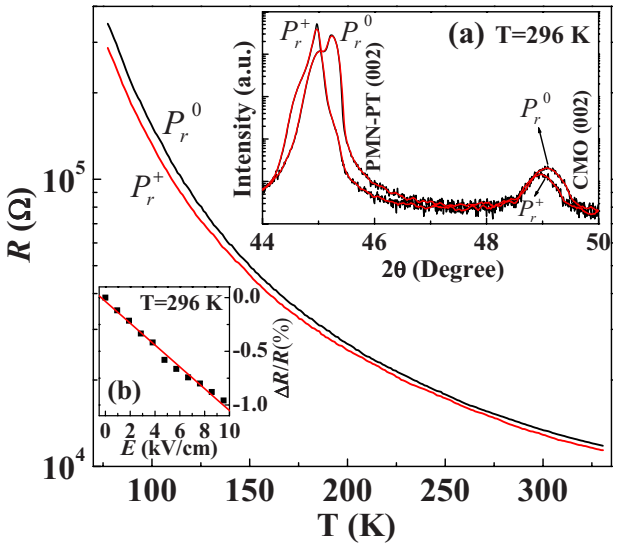

FIG. 7. (Color online) Temperature dependence of the resistance for the $CaMnO_3$ film under $H=0$ when the PMN-PT substrate is in P_r^0 and P_r^+ states, respectively. The inset (a) shows the XRD patterns for the $CaMnO_3$/PMN-PT structure when the PMN-PT substrate is in P_r^0 and P_r^+ states, respectively. The inset (b) shows the relative change of the resistance, $\Delta R/R$, of the $CaMnO_3$ film at 296 K as a function of E applied to the $CaMnO_3$/PMN-PT structure after the PMN-PT substrate had been polarized to P_r^+ state.

sile strain ε_{xx} is calculated to be reduced from 0.24% to 0.13%. As shown in Fig. 7, associated with the decrease in the in-plane tensile strain, the resistance in P_r^+ state becomes smaller than that in P_r^0 state in the whole temperature range. In order to get a clearer understanding of the strain effects in the $CaMnO_3$ film, we measured the resistance of the $CaMnO_3$ film by *in situ* reducing the in-plane tensile strain in the $CaMnO_3$ film via the converse piezoelectric effect after the PMN-PT substrate had been polarized to P_r^+ state. It can be seen in the inset (b) of Fig. 7 that the resistance decreases almost linearly with increasing E. Although the relative decrease in the resistance, $\Delta R/R$, is rather small, the results unambiguously show that a reduction in the in-plane tensile strain induced by the converse piezoelectric effect reduces the resistance of the $CaMnO_3$ film. Since the electronic bandwidth W can be estimated from the Mn-O bond length d and the Mn-O-Mn bond angle θ by using $W \propto \sin(\theta/2)/d^{3.5}$, a reduction in d would enhance W while a reduction in θ would reduce W. The effects of the induced strain on the resistance in the $CaMnO_3$ film demonstrate that the resistance change arising from the reduction in Mn-O bond length dominates over that arising from the reduction in Mn-O-Mn bond angle. We believe that this argument may be extended to the situation in LBMO films. The effect of the reduction in Mn-O bond length on the charge transport may also dominate over that of the reduction in the Mn-O-Mn bond angle in LBMO films.

IV. CONCLUSIONS

In summary, we examined the effects of substrate-induced strain on the strain state, resistance, and magnetotransport properties of LBMO and $CaMnO_3$ thin films by *in situ* modifying strain in the film via the ferroelectric poling or the converse piezoelectric effect. The ferroelectric poling or the converse piezoelectric effect substantially reduces the tensile strain in the film, giving rise to a reduction in the JT electron-lattice coupling and thus a large decrease in the resistance and an increase in T_C of the LBMO film. Quantitative relationships between the resistance and T_C, and the induced strain $\delta\varepsilon_{xx}$ in the LBMO film have been established. The induced strain $\delta\varepsilon_{xx}$ leads to opposite effects on MR below and above T_C, i.e., MR for $T<T_C$ is reduced while MR for $T>T_C$ is enhanced. We interpreted this behavior within the framework of the phase separation scenario relevant to the electron-lattice coupling linked to the strain induced by the ferroelectric poling. The results on $CaMnO_3$ film indicate that the strain-induced change of Mn-O bond length plays a more important role than that of Mn-O-Mn bond angle in influencing the transport properties of $CaMnO_3$ films. A similar scenario is anticipated in LBMO films.

ACKNOWLEDGMENTS

This work was supported by the Hong Kong Research Grants Council under Grant No. CERG PolyU 5122/07E and the Center for Smart Materials of the Hong Kong Polytechnic University.

*zrk@ustc.edu
†apahlcha@polyu.edu.hk

[1] T. Wu, S. B. Ogale, S. R. Shinde, Amlan Biswas, T. Polletto, R. L. Greene, and T. Venkatesan, J. Appl. Phys. **93**, 5507 (2003).
[2] S. I. Khartsev, P. Johnsson, and A. M. Grishin, J. Appl. Phys. **87**, 2394 (2000).
[3] F. Tsui, M. C. Smoak, T. K. Nath, and C. B. Eom, Appl. Phys. Lett. **76**, 2421 (2000).
[4] A. Biswas, M. Rajeswari, R. C. Srivastava, T. Venkatesan, R. L. Greene, Q. Lu, A. L. de Lozanne, and A. J. Millis, Phys. Rev. B **63**, 184424 (2001).
[5] R. Schmidt, Phys. Rev. B **77**, 205101 (2008).
[6] J. Zhang, H. Tanaka, T. Kanki, J. H. Choi, and T. Kawai, Phys. Rev. B **64**, 184404 (2001).
[7] T. Kanki, T. Yanagida, B. Vilquin, H. Tanaka, and T. Kawai, Phys. Rev. B **71**, 012403 (2005).
[8] X. J. Chen, S. Soltan, H. Zhang, and H.-U. Habermeier, Phys. Rev. B **65**, 174402 (2002).
[9] P. Murugavel, T. W. Noh, and J. G. Yoon, J. Appl. Phys. **95**, 2536 (2004).
[10] P. Murugavel, J. H. Lee, K. B. Lee, J. H. Park, J. S. Chung, J. G. Yoon, and T. W. Noh, J. Phys. D **35**, 3166 (2002).
[11] P. Murugavel, J. H. Lee, J. G. Yoon, T. W. Noh, J.-S. Chung, M. Heu, and S. Yoon, Appl. Phys. Lett. **82**, 1908 (2003).

[12] P. Orgiani, A. Guarino, C. Aruta, C. Adamo, A. Galdi, A. Yu. Petrov, R. Savo, and L. Maritato, J. Appl. Phys. **101**, 033904 (2007).
[13] H. Cao, F. M. Bai, J. F. Li, D. Viehland, G. Y. Xu, H. Hiraka, and G. Shirane, J. Appl. Phys. **97**, 094101 (2005).
[14] C. H. Ahn, R. H. Hammond, T. H. Geballe, M. R. Beasley, J.-M. Triscone, M. Decroux, Ø. Fischer, L. Antognazza, and K. Char, Appl. Phys. Lett. **70**, 206 (1997).
[15] M. K. Lee, T. K. Nath, C. B. Eom, M. C. Smoak, and F. Tsui, Appl. Phys. Lett. **77**, 3547 (2000).
[16] R. B. Gangineni, L. Schultz, C. Thiele, I. Mönch, and K. Dörr, Appl. Phys. Lett. **91**, 122512 (2007).
[17] C. Thiele, K. Dörr, S. Fähler, L. Schultz, D. C. Meyer, A. A. Levin, and P. Paufler, Appl. Phys. Lett. **87**, 262502 (2005).
[18] C. Thiele, K. Dörr, O. Bilani, J. Rödel, and L. Schultz, Phys. Rev. B **75**, 054408 (2007).
[19] R. K. Zheng, Y. Wang, H. L. W. Chan, C. L. Choy, and H. S. Luo, Appl. Phys. Lett. **90**, 152904 (2007).
[20] R. K. Zheng, Y. Wang, J. Wang, K. S. Wong, H. L. W. Chan, C. L. Choy, and H. S. Luo, Phys. Rev. B **74**, 094427 (2006).
[21] R. K. Zheng, J. Wang, X. Y. Zhou, Y. Wang, H. L. W. Chan, C. L. Choy, and H. S. Luo, J. Appl. Phys. **99**, 123714 (2006).
[22] H. S. Luo, G. S. Xu, H. Q. Xu, P. C. Wang, and Z. W. Yin, Jpn. J. Appl. Phys., Part 1 **39**, 5581 (2000).
[23] P. G. Radaelli, M. Marezio, H. Y. Hwang, and S.-W. Cheong, J. Solid State Chem. **122**, 444 (1996).
[24] T. Kanki, Y. G. Park, H. Tanaka, and T. Kawai, Appl. Phys. Lett. **83**, 4860 (2003).
[25] Y. F. Lu, J. Klein, C. Höfener, B. Wiedenhorst, J. B. Philipp, F. Herbstritt, A. Marx, L. Alff, and R. Gross, Phys. Rev. B **62**, 15806 (2000).
[26] X. J. Chen, H.-U. Habermeier, H. Zhang, G. Gu, M. Varela, J. Santamaria, and C. C. Almasan, Phys. Rev. B **72**, 104403 (2005).
[27] A. J. Millis, T. Darling, and A. Migliori, J. Appl. Phys. **83**, 1588 (1998).
[28] N. M. Souza-Neto, A. Y. Ramos, H. C. N. Tolentino, E. Favre-Nicolin, and L. Ranno, Appl. Phys. Lett. **83**, 3587 (2003).
[29] N. M. Souza-Neto, A. Y. Ramos, H. C. N. Tolentino, E. Favre-Nicolin, and L. Ranno, Phys. Rev. B **70**, 174451 (2004).
[30] R. K. Zheng, Y. Wang, H. L. W. Chan, C. L. Choy, and H. S. Luo, Appl. Phys. Lett. **92**, 082908 (2008).
[31] S. W. Jin, G. Y. Gao, Z. Z. Yin, Z. Huang, X. Y. Zhou, and W. B. Wu, Phys. Rev. B **75**, 212401 (2007).
[32] L. Sudheendra, V. Moshnyaga, and K. Samwer, Contemp. Phys. **48**, 349 (2007).
[33] D. Gillaspie, J. X. Ma, H. Y. Zhai, T. Z. Ward, H. M. Christen, E. W. Plummer, and J. Shen, J. Appl. Phys. **99**, 08S901 (2006).
[34] Z. Zeng, M. Greenblatt, and M. Croft, Phys. Rev. B **59**, 8784 (1999).